Science of the Total Environment 691 (2019) 908–918

Contents lists available at ScienceDirect

Science of the Total Environment

journal homepage: www.elsevier.com/locate/scitotenv

Interplay between resistance and resilience governs the stability of a freshwater microbial food web under multiple stressors

Marco J. Cabrerizo [a,b,*], Juan Manuel Medina-Sánchez [b], Manuel Villar-Argaiz [c], Presentación Carrillo [b,**]

[a] Departamento de Ecología y Biología Animal, Facultad de Ciencias del Mar, Campus Lagoas Marcosende s/n, 36310 Vigo, Spain
[b] Instituto Universitario de Investigación del Agua, Universidad de Granada, C/ Ramón y Cajal, 4, 18071 Granada, Spain
[c] Departamento de Ecología, Facultad de Ciencias, Universidad de Granada, Campus Fuentenueva s/n, 18071 Granada, Spain

HIGHLIGHTS

- Multiple stressor impacts on the stability of microbial food webs were investigated.
- A complex scenario increased the resilience of phototrophs vs. mixo and heterotrophs.
- The ecosystem's metabolic balance was strongly resistant to multi-stressor impacts.
- A high resilience of phototrophs maintained the carbon sink capacity of the ecosystem.

GRAPHICAL ABSTRACT

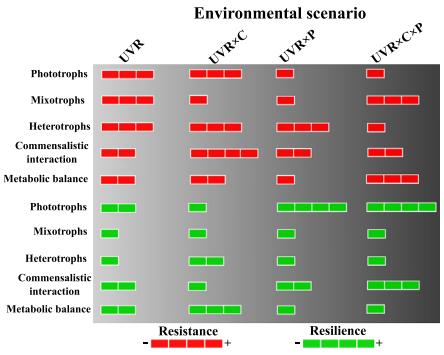

ARTICLE INFO

Article history:
Received 22 May 2019
Received in revised form 9 July 2019
Accepted 11 July 2019
Available online 12 July 2019

Editor: Daniel Wunderlin

Keywords:
Metabolic balance
Multiple stressors
Oligotrophic ecosystems
Phytoplankton-bacteria interaction
Resilience
Resistance

ABSTRACT

Energy (photosynthetically active [PAR] and ultraviolet [UVR] radiation) and matter (organic and inorganic nutrients) fluxes regulate the ecosystem's stability. However, the mechanisms underpinning the potential interplay between resistance and resilience to shifts in nutrient inputs and UVR are poorly understood. To assess how the UVR × nutrients interaction alters ecosystem stability, we exposed in situ a microbial food web from an oligotrophic ecosystem to: (1) two light (UVR + PAR and PAR), and (2) four nutrient (ambient concentrations, phosphorus [P], carbon [C] and C × P addition) treatments for three weeks. During this period, we quantified the community composition and biomass, sestonic P and C:P ratio, primary [PP] and bacterial [BP] production, community [CR] and bacterial [BR] respiration, excreted organic carbon [EOC], as well as the commensalistic phytoplankton-bacteria interaction (i.e. bacterial carbon demand [BCD]:EOC ratio) and the metabolic balance of the ecosystem (i.e. [PP:R] ratio). The stability of all response variables under the four environmental scenarios tested (i.e. UVR, UVR × C, UVR × P, and UVR × C × P) was quantified by means of the resistance and resilience indexes. The microbial community was dominated by phototrophs during the experimental period regardless of the treatment considered. The most complex scenario, i.e. UVR × C × P, decreased the resistance for all variables, except for BR and the PP:R ratio. Despite that PP:R ratio showed the highest resistance under such scenario, it was >1 in all environmental scenarios (i.e. net autotrophic), except under the UVR × C interaction, where, concomitant with increased resilience, the balance shifted towards net heterotrophy (PP:R < 1). Under the UVR × C × P scenario, the metabolic balance of the ecosystem proved strongly resistant due mainly to high resistance of

* Correspondence to: M. J. Cabrerizo, Departamento de Ecología y Biología Animal, Facultad de Ciencias del Mar, Campus Lagoas Marcosende s/n, 36310 Vigo, Spain.
** Corresponding author.
E-mail addresses: marcojc@uvigo.es (M.J. Cabrerizo), jmmedina@ugr.es (J.M. Medina-Sánchez), mvillar@ugr.es (M. Villar-Argaiz), pcl@ugr.es (P. Carrillo).

https://doi.org/10.1016/j.scitotenv.2019.07.173

bacterial respiration and a firm stability of the commensalistic interaction. Our results evidence that the high resilience of phototrophs (favoring their predominance over mixo- and heterotrophs) may lead to the maintenance of the autotrophic nature and carbon (C) sink capacity of the ecosystem.

1. Introduction

Aquatic ecosystems are among the main biodiversity reserves (Dudgeon et al., 2006) and the most important sinks of carbon (C) on Earth, thus might potentially mitigate climate change (Mendonça et al., 2018). In these ecosystems, the microbial food web plays a crucial role in regulating diverse functions such as, nutrient and organic matter (re)cycling, trophic interactions, or gas exchanges in the atmosphere-water interphase (Mostajir et al., 2015). Within microbial food webs, phytoplankton constitutes the base, responding rapidly to environmental changes, particularly nutrient loading. In fact, recent evidence shows that the increasing nutrient inputs into ecosystems (nitrogen [N], phosphorus [P]) are lowering phytoplankton C:N and C:P ratios, accelerating the algal growth rates, and improving food quality for consumers (Bergström et al., 2018; Villar-Argaiz et al., 2018). In addition, the input of limiting nutrients to aquatic ecosystems reduces the competition between phytoplankton and bacteria, stimulating the growth of both (Danger et al., 2008; Carrillo et al., 2008a). This positive effect on both communities, and the reported increase in the excretion of photosynthetic organic carbon (EOC), reinforce the commensalistic phytoplankton-bacteria coupling (Medina-Sánchez et al., 2013; Durán et al., 2016). The coupling, defined as the capacity of the EOC to support the bacterial carbon demand (BCD, Morán et al., 2002), is modulated by interacting global-change drivers such as UVR and stratification (Carrillo et al., 2015), or UVR and warming (Durán et al., 2016). Hence, changes in the coupling of this interaction (BCD:EOC > or < 1) modulates the C flux from the microbial loop to the grazing chain (Medina-Sánchez et al., 2004; Degerman et al., 2018) and might modify the metabolic balance (i.e. production:respiration [PP:R] ratio) in aquatic ecosystems. This ratio can be upset either towards less PP than R when the nutrient inputs are land-derived organic C (Ask et al., 2012) or towards more PP than R when the dominant inputs are dissolved inorganic nutrients (Bogard et al., 2017).

Two key facets of ecosystem stability are: (1) resistance, defined as the ability of a community to remain unaltered after an external disturbance and (2) resilience, defined as the ability of a community to recover from an external disturbance (Russell and Connell, 2014). Recent studies have suggested that terrestrial communities dominated by slower-growing organisms (i.e. fungi) tend to be more resistant than those dominated by faster-growing organisms (i.e. bacteria) when undergoing disturbances; however, the former also tend to being less resilient (Allison and Martiny, 2008; de Vries et al., 2012).

Despite the ecological relevance that the ecosystem's stability (and of their communities) has in a global-change context, almost 90% of the studies have assessed only one facet of stability, about 80% of them have measured the impact of a single stressor, and only some 2% have examined the stability of an ecosystem's functions or processes (Donohue et al., 2016). Moreover, Donohue et al. (2016) have shown that roughly 75% of the studies on ecological stability concern terrestrial ecosystems. Thus, we currently lack sufficient quantification of the main components (resistance, resilience) of ecological stability in aquatic ecosystems. This is partly because most of researchers have focused on the immediate response of the community to such perturbations, thus neglecting how microbial aquatic communities respond after exposure to a stressor over time (Garnier et al., 2017; Shade et al., 2011). Furthermore, little is known concerning how resistance and resilience could be affected in natural ecosystems by interacting global-change stressors. The few studies dealing with the impacts of multiple stressors on stability come from laboratory experiments under unrealistic environmental conditions and using cultured species in isolation or pairs of interacting species (Mayali, 2018; Ramanan et al., 2016). Only recently, results from mesocosm studies by Baert et al. (2016) and Flöder and Hillebrand (2012) have evidenced that the exposure of aquatic communities to one stressor hampers the system's ability to stabilize ecosystem functions against other stressors, mainly because the various species of a community can have different tolerance ranges for a given stressor.

The above reflects the need for experimental in situ studies quantifying: (1) the compartment of the microbial food web that is most resistant to interacting stressors; (2) how the stability of the commensalistic phytoplankton-bacteria interaction is altered under interacting stressors; and (3) how the stability of the metabolic balance of the ecosystem is altered under future environmental scenarios of increased nutrient concentrations (i.e. C and/or P) and high UVR levels expected under the RCP8.5 scenario by the end of this century (IPCC, 2013).

To address these issues, we test, for the first time, how C and/or P inputs under high UVR alter the stability of the microbial community using stoichiometric, structural, metabolic, and trophic approaches. Also we examine how this alteration influences the stability of metabolic balance (PP:R ratio) of the ecosystem. Our working hypotheses was that, under a UVR × C × P scenario, a greater resistance of phytoplankton compared to bacteria will maintain or strengthen their commensalistic interaction, maintaining or bolstering the autotrophic metabolic balance of the ecosystem.

2. Material and methods

2.1. Experimental setup

A mesocosm experiment was conducted on PVC-customized floating platforms set in the water of La Caldera, an oligotrophic Mediterranean high-mountain lake situated above the treeline (3050 m.a.s.l.) in the Sierra Nevada National Park (Southern Spain, 36°55′–37°15′N, 2°31′–3°40′W). This system has been used in several studies related to the impact of global-change stressors on plankton communities over recent decades (Cabrerizo et al., 2017; Carrillo et al., 2008b; Villar-Argaiz et al., 2001). The experiment lasted from 31 August (day 0) to 18 September 2011. A total of 24 transparent semi-spherical polyethylene bags (mesocosms, 0.58 m diameter) were each filled with 100 L of surface water (from 0.2 to 0.5 m depth) pumped directly from the lake. The water was sieved through 45-μm pore mesh to exclude metazooplankton and because phytoplankton cell size is smaller than this size in Lake La Caldera, and mixed before and after nutrient additions. Mesocosms were placed at 1 m in depth to mimic the worst-case UVR scenario with a shallower upper mixed layer, in such a way that communities received mean solar irradiance 2- to 3-fold higher than received in the water column (Cabrerizo et al., 2017). The volume of mesocosms was sufficient to minimize the bottle effect over the experimental period (Dorado-García et al., 2014).

The experiment had a 2 × 4 design in triplicate with two radiation levels: 1) **PAB** (>280 nm; uncovered mesocosms) and 2) **PAR** (>400 nm; mesocosms covered with UV-filter foil which block UVR). It also had four nutrient levels: 1) Ambient (**Amb**, non-enriched mesocosms), 2) **C** (addition of 290.2 μM), 3) **P** (addition of ~1 μM), and 4) **C** × **P** (addition of both at the same concentration than mentioned above) (Fig. 1). The PAB_{amb} treatment represented the control

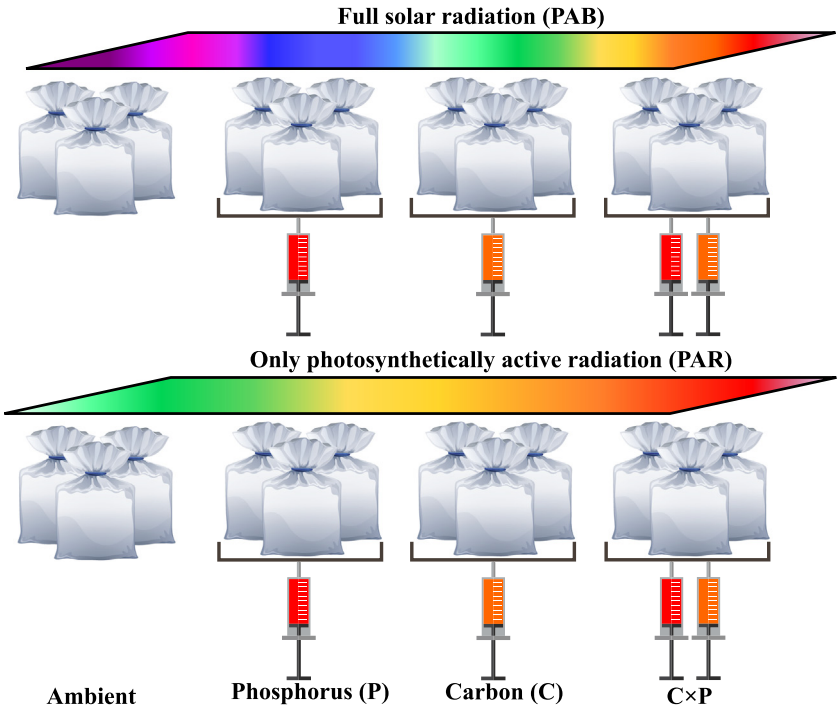

Fig. 1. Graphical scheme of the experimental design in which natural plankton communities were exposed to radiation (PAB [>280 nm] and PAR [>400 nm]) and nutrient additions (ambient concentrations, carbon [C], phosphorus [P], and C × P) (see a detailed description in Material and methods section).

conditions for testing the net effect of UVR, nutrients, and their interaction (see below). The C and P were added once at the beginning of the experiment as sucrose and Na_2HPO_4, respectively. These concentrations were selected to ensure nutrient availability over the experimental period, maintaining a N:P molar ratio of 30 in P-enriched mesocosms, and a C:P molar ratio of 300 in C-enriched mesocosms (C and C × P). Additionally, to maintain the N:P ratio, 30 μM of NH_4NO_3 were added. Such nutrient additions were setup to mimic the mean TN:TP ratios found in natural atmospheric deposition events on Lake La Caldera (Morales-Baquero et al., 2006). For ambient nutrient treatments, the N:P ratio was those found in the lake at the beginning of the experimental setup (i.e. ~350). All samples used in the incubations were taken using a water pump connected to an acid-washed silicone tube inserted into each mesocosm. Samples for nutrient and chlorophyll *a* (Chl *a*) analyses and taxonomic identification of components of the plankton communities were taken every 3–5 days, whereas those related to stoichiometric and metabolic variables (see below) were taken at two specific times over the experiment, i.e. on the fifth day (hereafter, "at the pulse") and on the last experimental day (hereafter, "after the pulse period"). These periods were established according to previous results by Dorado-García et al. (2014) who found that a 4-day period is necessary to measure any detectable change both in phyto- and bacteria communities in Lake La Caldera.

2.2. Physical and chemical parameters

Vertical profiles of temperature, pH, and conductivity of Lake La Caldera were done during the sampling using a multiparametric probe (Hanna HI9828-O, USA), whereas that the underwater irradiance was measured with a BIC compact 4-channel radiometer (Biospherical Instruments, CA, USA).

Samples (25 mL) for total dissolved nitrogen (TDN) and phosphorus (TDP) were digested with persulfate following the methodology of APHA (2017), and measured as soluble reactive P (SRP) by applying the acid molybdate technique in the case of TDP, and as nitrate for TDN. Samples (100 mL) for dissolved organic carbon (DOC) were filtered through pre-combusted GF/F Whatman filters, acidified with HCL 2N final concentration, and stored in darkness at 4 °C until analysis (Reche et al., 2001). The DOC concentration was measured using the high-temperature catalytic oxidation method in a Shimadzu TOC analyzer (model 5000) (Benner and Strom, 1993).

2.3. Sestonic P and C

Water samples (500 mL) were filtered through pre-combusted GF/B Whatman filters, placed in acid-washed vessels, and either persulfate digested for 30 min at 120 °C and measured as SRP in the case of sestonic P (APHA, 2017), or dried for 24 h at 60 °C, and analyzed using an elemental analyzer (Perkin Elmer, 2400, USA) as occurred for sestonic C.

2.4. Chlorophyll a

Samples (250 mL) for phytoplankton pigment analysis were filtered through GF/F Whatman filters under a vacuum pressure of <75 mm Hg and in dim light. The filters were placed in centrifuge tubes with 5 mL of 90% acetone for 24 h at 4 °C in darkness. Chl *a* was measured fluorimetrically with a Perkin Elmer LS55 (USA) fluorometer routinely calibrated with pure spinach Chl *a* (Sigma Aldrich, USA), and the concentration was estimated using the equation of Jeffrey and Humphrey (1975).

2.5. Phytoplankton and heterotrophic bacteria biomass

Total abundance of phytoplankton was quantified following the methodology of Straškrabová et al. (1999), whereas bacterial abundance was measured using flow cytometry (FACSCanto II, Becton Dickinson Biosciences, Oxford, UK). Briefly, before flow-cytometry measurements, 1.5 mL of sample was fixed with particle-free 20% (w/v) paraformaldehyde (75 μL, 1% final concentration), frozen in liquid nitrogen, and stored at −80 °C until analyzed (Kamiya et al., 2007; Zubkov et al., 2007). Phytoplankton and heterotrophic bacteria biomass were estimated approximating the cell volume to their geometric shape (phytoplankton, Hillebrand et al., 1999; bacteria, Zubkov et al., 2007; Zubkov and Burkill, 2006), and the results were transformed to C units

(phytoplankton, Rocha and Duncan, 1985; bacteria, Posch et al., 2001). For ciliates and heterotrophic nanoflagellates (HNFs), an aliquot of 300 mL of sample was settled for 72 h, and the supernatant was removed by suction using a Pasteur pipette coupled to a low-pressure pump. The remaining volume was again settled in an Utermöhl chamber with the same procedure as described above. Because some phytoplankton groups in Lake La Caldera are mixotrophic (see Cabrerizo et al., 2017), we grouped phytoplankton into two functional groups, i.e. phototrophs and mixotrophs, while bacteria were considered heterotrophs.

2.6. Phytoplankton and heterotrophic bacterial production

Primary production (PP) was quantified using the ^{14}C-incorporation method (Steemann Nielsen, 1952). A total of 64 experimental samples (i.e. 32 at the pulse and 32 after the pulse period, constituting three light plus one dark control per experimental treatment), were placed in 50-mL quartz vessels, inoculated with 5 μCi of radiolabelled sodium bicarbonate (Perkin Elmer, Inc. USA.), and incubated in situ at the same depth as the microcosm for 4 h centered at noon. Before filtration, 4 mL were taken to measure the total organic carbon (TOC). Particulate PP was determined by filtering an aliquot of 45 mL through 1.0-μm pore-size Nucleopore filters 25 mm in diameter. To minimize cell breakage, we applied low pressure (<100 mm of Hg). The filters were placed in scintillation vials and the DI^{14}C was removed by adding 100 μL of 1 N HCl. The filtrate [<1 μm, excretion of organic carbon (EOC)] was also collected and treated as described above for the TOC (more details in Carrillo et al., 2002). From total PP (as the sum of PP + EOC) and community respiration (CR, see below), we quantified the primary production:respiration (PP:R) ratio at the pulse and after the pulse period.

Heterotrophic bacterial production (BP) was measured using the ^{3}H-thymidine-incorporation method (Fuhrman and Azam, 1982). A total of 80 samples of 1.5 mL (i.e. 40 at the pulse and 40 after the pulse period, three light plus two blank controls per experimental treatment) were placed in acid-cleaned and sterilized microtubes, inoculated with ^{3}H-thymidine (SA = 48–50 Ci mmol^{-1}, Perkin Elmer) to a final saturating concentration of 12 nM, and incubated in situ in darkness for 1 h. Trichloroacetic acid (TCA, 5% final concentration) was used for extraction. After this, microtubes were centrifuged at 16000*g*, rinsed twice with 5% TCA, and measured in a scintillation counter (Beckman LS 6000TA). A conversion factor of 1×10^{8} cells mol^{-1} of thymidine and 2×10^{-14} g C cell^{-1} was applied to convert incorporated ^{3}H-thymidine rates into BP rates in terms of C (Posch et al., 2001).

2.7. Bacterial carbon demand and bacterial growth efficiency

Bacterial carbon demand (BCD) was calculated as the sum of BP and BR (del Giorgio and Cole, 1998; Vidal et al., 2011). As the organic carbon excreted by phytoplankton constitutes the C source preferentially used by bacteria (Durán et al., 2016), and given the feasibility of segregating the microbial fraction in Lake La Caldera by filtration (Medina-Sánchez et al., 2002), we calculated the strength of commensalistic phytoplankton-bacteria interaction as BCD divided by EOC.

2.8. Respiration

Samples (35 mL) to quantify community (CR) and bacterial (BR) respiration were placed in glass vessels equipped with optode sensor-spots (SP-PSt3-NAU-D5-YOP) and incubated in darkness in a temperature-controlled bath to maintain the same temperature as in the lake. For BR measurements, samples were previously filtered through GF/F Whatman filters to eliminate the fraction >0.7 μm. The oxygen concentration [O_2] was measured using an optic-fiber oxygen transmitter (Fibox 3; PreSens GmbH, Germany) equipped with Oxyview 6.02 software to register the data. Each sample was measured for 30 s, collecting one datum per second. Before the measurements, the transmitter was calibrated using a two-point (0 and 100% saturation) calibration procedure, at the in situ temperature while taking into account the atmospheric pressure. The CR and BR rates (in oxygen units) were calculated from least-square regressions [O_2] vs. time and expressed in μg C L^{-1} h^{-1} assuming a respiratory quotient of 1 (del Giorgio and Cole, 1998).

2.9. Calculations and statistical analysis

The diversity of the phytoplankton community for each experimental treatment, at the pulse and after the pulse period, was quantified according to the Shannon-Weaver index (H′; Shannon and Weaver, 1949).

The resistance and resilience indexes were quantified for planktonic groups (photo-, mixo-, and heterotrophs biomass), metabolic processes (PP, BP, EOC, CR, and BR rates), commensalistic interaction (BCD:EOC ratio), metabolic balance of ecosystem (PP:R ratio) and biodiversity of the phytoplankton community following the methodology of Orwin and Wardle (2004).

Resistance index was calculated as:

$$\text{Resistance} = 1-(2 \mid D_0 \mid /(C_0 + |D_0|)$$

where C_0 is the value of the control at the pulse, in this case P_{Amb}; and $|D_0|$ is the absolute difference between the control and the perturbed treatment during the same period, in this case, PAB_{Amb} for the UVR effects, PAB_C for the UVR × C, PAB_P for the UVR × P, and $PAB_{C\times P}$ for the UVR × C × P interaction.

The resilience index was calculated as:

$$\text{Resilience} = (2|D_0|)/(|D_0| + |D_x|)-1$$

where $|D_x|$ is the absolute difference between the control and the perturbed treatment (i.e. those described above) after the pulse period (i.e. the last experimental day).

For each index, a value of +1 indicates that the perturbation had no effect (maximal resistance) or a full recovery (maximal resilience) of the response variable considered, whereas a value lower than +1 indicates less resistance or a slower recovery rate. We used these indexes because they provide a quantitative measure of both the resistance and resilience of a response variable in all environmental scenarios. This enables us to determine the relative contribution of each component to the stability of the ecosystem.

A two-way analysis of variance (ANOVA) was used to test the interaction between radiation and nutrients at the pulse and after the pulse period on stoichiometry (sestonic C and P, and C:P ratio), metabolic processes, commensalistic interaction and metabolic balance of ecosystem. A one-way ANOVA was used to test the effect of the environmental scenario (four levels: UVR, UVR × C, UVR × P, and UVR × C × P) on the resistance and resilience indexes of the metabolic processes, commensalistic interaction, and metabolic balance of ecosystem. Significant differences among treatments were assessed with a Tukey HSD post hoc test.

Also, a one-way repeated measures ANOVA was used to test the effect of the environmental scenario (four levels: UVR, UVR × C, UVR × P and UVR × C × P) (between factors) and the photo-, mixo- and heterotrophs (within factor) on the resistance and resilience indexes calculated for biomass of functional groups. As above, significant differences were assessed with a Tukey HSD post hoc test. Due to the multiple comparisons between environmental scenarios for resistance and resilience indexes, it was impractical to add symbols to the figures to indicate all possible significances; thus, we mentioned in the text the essential comparisons, adding the significance when needed. A linear regression analysis was used to assess the relationship between compositional (i.e. diversity) and metabolic (i.e. PP) stability (resistance or resilience). Assumptions of normality of the residuals (by

Kolmogorov-Smirnov and Shapiro-Wilk's tests) and homoscedasticity (by Levene's test) were checked both for ANOVA and linear regression analyses. When these parameters were not met, they were log transformed. Statistical analyses were made using the R environment v. 3.4.4 (https://cran.r-project.org).

3. Results

3.1. Abiotic environment: lake and experimental conditions

In the water column the physical conditions and optical properties of Lake La Caldera showed a gradual decline in temperature from surface to bottom, and a high transparency to both UVR ($Kd_{305} = 0.61$, $Kd_{320} = 0.53$, $Kd_{380} = 0.52$) and PAR ($Kd = 0.25$). The pH values ranged between 8.33 and 9.14, whereas the conductivity did not vary along the water column (19.85 ± 0.80 μS cm^{-1}). Likewise, the DOC concentration also remained constant (49.38 ± 2.71 μM; Fig. S1) with low TDP and TDN concentrations that became undetectable over the experimental period.

For the experiment, in ambient nutrient treatments, no major changes were found in TDP (values <1 μM), TDN (values <20 μM, except the last two days in P_{Amb} ~50 μM) or DOC (values <100 μM; Fig. S1A–C) concentrations. Conversely, in the P and C × P treatments, TDP slightly increased regardless of the radiation treatment up to day 10 (values 0.2–0.9 μM). From this day, a slight decline in TDP was found, being such decrease greater under the PAR than the PAB treatment. As for TDP, DOC increased in values up to day 9 (values >200 μM) in P and C × P treatments, maintaining these values only in C × P treatments at the end of the experiment. In C treatments, DOC values dropped to concentrations similar to those in the ambient treatment regardless the radiation treatment considered (Fig. S1). The TDN concentrations showed no clear response pattern in any treatment along the experiment (Fig. S1).

3.2. Structural responses of the microbial food web

Chl *a* followed two well-differentiated patterns among treatments: (1) low concentrations under ambient and C treatments over the experiment (mean values ~3.17 and 2.76 μg L^{-1}, respectively); and (2) increased concentrations (up to one order of magnitude) in P and C × P treatments, these being significantly (Tukey HSD, $p < 0.05$) higher in $PAB_{C\times P} > PAB_P > PAR_{C\times P} > PAR_P$ treatments after the pulse period (Fig. S1D).

The structure of the microbial community was dominated mostly by phytoplankton in all treatments, with mean biomass ranging between ~40 (Amb and C-treatments) and ~240 μg C L^{-1}(P and C × P treatments). Heterotrophic bacteria biomass remained <15 μg C L^{-1} under all the experimental conditions (Fig. 2). Nevertheless, whereas the phototrophs (mainly Chlorophyceae, *Monoraphidium* sp.) showed no clear response under the ambient and C treatments, they followed a domed-curve dynamic under the P and C × P-treatments. The response pattern observed matched an increase in mixotroph biomass (mainly Chrysophyceae, *Chromulina nevadensis*; Fig. 2C), particularly in the P-treatment when available TDP concentrations became low after day 16. Bacillariophyceae (i.e. *Cyclotella* sp.), Dinophyceae (i.e. *Gymnodinium* sp.), Cryptophyceae (i.e. *Rhodomonas* and *Cryptomonas* sp.), and Desmidiaceae (i.e. *Cosmarium* sp.) represented <5% of the total biomass in all the treatments. No ciliates or HNFs were detected in any treatment throughout the experiment.

Sestonic C registered the highest values (>500 μg L^{-1}) in the C × P treatments without significant differences among the other treatments (values <400 μg L^{-1}) after the pulse period (Fig. S2A; Table S1). By contrast, sestonic P reached the highest values in the P and C × P treatments at the pulse, but fell afterwards. No significant differences were found in the ambient or C treatments regardless of the radiation treatment and experimental period (Fig. S2B). Regarding the sestonic C:P ratio, significantly lower values were found in P and C × P (<400) than in the ambient and C (>500) treatments, particularly at the pulse (Fig. S2C; Table S1).

3.3. Metabolic responses of the microbial food web

PP, BP, EOC, and BCD were significantly higher under P and C × P than under ambient and C treatments (Fig. 3; Table S1) regardless of the period considered. Overall, UVR exerted a significant inhibitory effect on all the aforementioned variables, except on BP ($PAB_{C\times P}$ vs. $PAR_{C\times P}$; Fig. 3B) and EOC (PAB_P vs. PAR_P; Fig. 3E), which proved stimulatory after the pulse period. Respiratory variables, i.e. CR and BR (Fig. 3C–D), showed the greatest values under the C × P treatments, particularly at the pulse. UVR exerted an inhibitory effect on both respiratory variables at the pulse but this effect dissipated after the pulse period (Fig. 3C, D).

3.4. Strength of the commensalistic interaction and metabolic balance of the ecosystem

Regarding the C demand vs. C supply, under PAB_P and $PAB_{C\times P}$ treatments, EOC satisfied the BCD regardless of the period considered (Fig. 3G). By contrast, under PAB_C, BCD was 8-fold higher than EOC after the pulse period (Fig. 3E, F). This response by the Rad×Nut interaction was translated into a shift from a metabolic balance (PP:R ~1) at the pulse to a net heterotrophy (PP:R < 1) after the pulse period (Fig. 3H). In the remaining treatments, we found that the P and C × P addition enhanced autotrophy (up to 8-fold) compared to ambient conditions at the pulse and after the pulse period.

3.5. Stability of the microbial food web

Figs. 4 and 5 plot the resistance and resilience indexes for: (1) functional groups (Fig. 4A, B), metabolic processes (Fig. 4C–F), commensalistic interaction and metabolic balance of ecosystem (Fig. 5A, B) under four environmental scenarios of increasing complexity by the number of interacting stressors (i.e. UVR, UVR × C, UVR× P, and UVR × C × P).

First, at a functional group level, our findings show that under UVR all of them reached high resistance values (c. 0.7), without significant differences among groups (Fig. 4A; Table S2). The addition of C and P, both individual and in combination, under UVR reduced the resistance in all groups with the lowest values in: 1) phototrophs under UVR × P (−0.5); 2) mixotrophs under UVR × C and UVR × P (~0), but without changes under UVR × C × P; 3) and heterotrophs under UVR × C × P (−0.25). The resilience of the different functional groups clearly responded with high and even maximal resilience values for phototrophs under UVR, UVR × P, and UVR × C × P, matching minimal resilience values for mixotrophs and heterotrophs (Tukey HSD post hoc, $p < 0.05$; Fig. 4B). Likewise, conditions of maximal resilience of heterotrophic bacteria coincided with lower resilience values of photo- and mixotrophs, as occurred under the UVR × C scenario (Fig. 4B).

Second, a contrasting response appeared in the resistance of phytoplanktonic and bacterial metabolic variables (Fig. 4C–F; Table S3). Thus, PP, EOC, and CR exhibited significantly diminishing resistance (values ranging from 0.41 to – 0.50; Tukey HSD post hoc, $p < 0.001$) with increasing complexity of the environmental scenario (Fig. 4C). This decrease resulted in a slight increase in the resilience for EOC and CR, but not of PP, as such values were significantly lower under the UVR × C × P than UVR and UVR × C scenarios (Tukey HSD post hoc, $p < 0.05$; Fig. 4D). The resistance index of BP and BR was 3-fold higher under UVR × P and UVR × C × P than under the other two scenarios (except in BP, Fig. 4E), and matched the respective lowest resilience values (Fig. 4F). Noticeably, BR showed maximal resistance values (~1) under the UVR × P and UVR × C × P scenarios (Tukey HSD post hoc, $p < 0.05$).

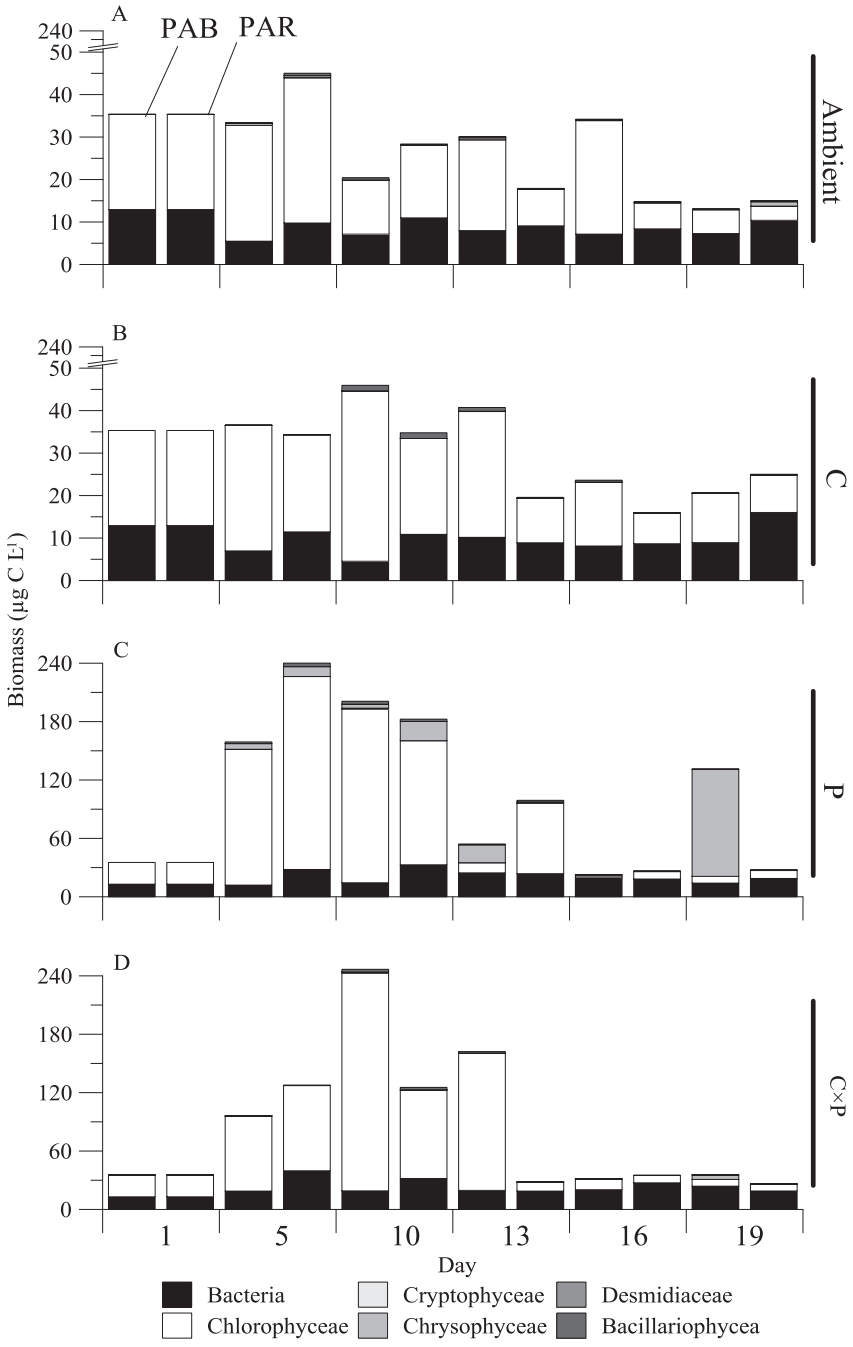

Fig. 2. Temporal dynamics of the phytoplankton groups and bacteria (in µg C L^{-1}) during the incubation period in each radiation (PAB [>280 nm] and PAR [>400 nm]) and nutrients (ambient, carbon [C], phosphorus [P] and C × P) treatment.

Third, at the commensalistic interaction level, the highest resistance of BCD:EOC ratio was found under the UVR × C scenario, coinciding with their lowest resilience values. By contrast, under UVR × C × P scenario the BCD:EOC ratio showed low resistance, but the highest of resilience values (Fig. 5A, B solid symbols; Table S4). An opposite response pattern to BCD:EOC ratio was found in the metabolic balance of ecosystem (PP:R ratio), which showed the highest resistance values but the lowest resilience values under a UVR × C × P scenario (Fig. 5A, B open symbols; Table S4). UVR × C scenario only generated a significant (Tukey HSD post hoc, $p < 0.05$) increase of resilience of the PP:R ratio.

Finally, regarding the relationship between compositional (i.e. diversity) and metabolic (i.e. PP) stability under the four environmental scenarios tested, no correlation was found between the two variables when the resistance was considered (Fig. 6A). Conversely, a significant negative relationship ($R^2 = 0.32$; F, $p < 0.001$) was found between the resilience of the two variables (Fig. 5B).

4. Discussion

This study constitutes the first empirical study that evaluates the resistance and the resilience of aquatic microbial food webs facing simultaneous pulses of C and P under UVR, key stressors related to global change. Our main result was that the metabolic balance of the ecosystem (PP:R) was strongly resistant to the UVR × C × P scenario. This response was related mainly to a high resistance of bacterial respiration as well as a strong stability of the commensalistic interaction linked to an enhanced EOC derived from higher PP rates. Below, this striking response is discussed by posing three key issues concerning the

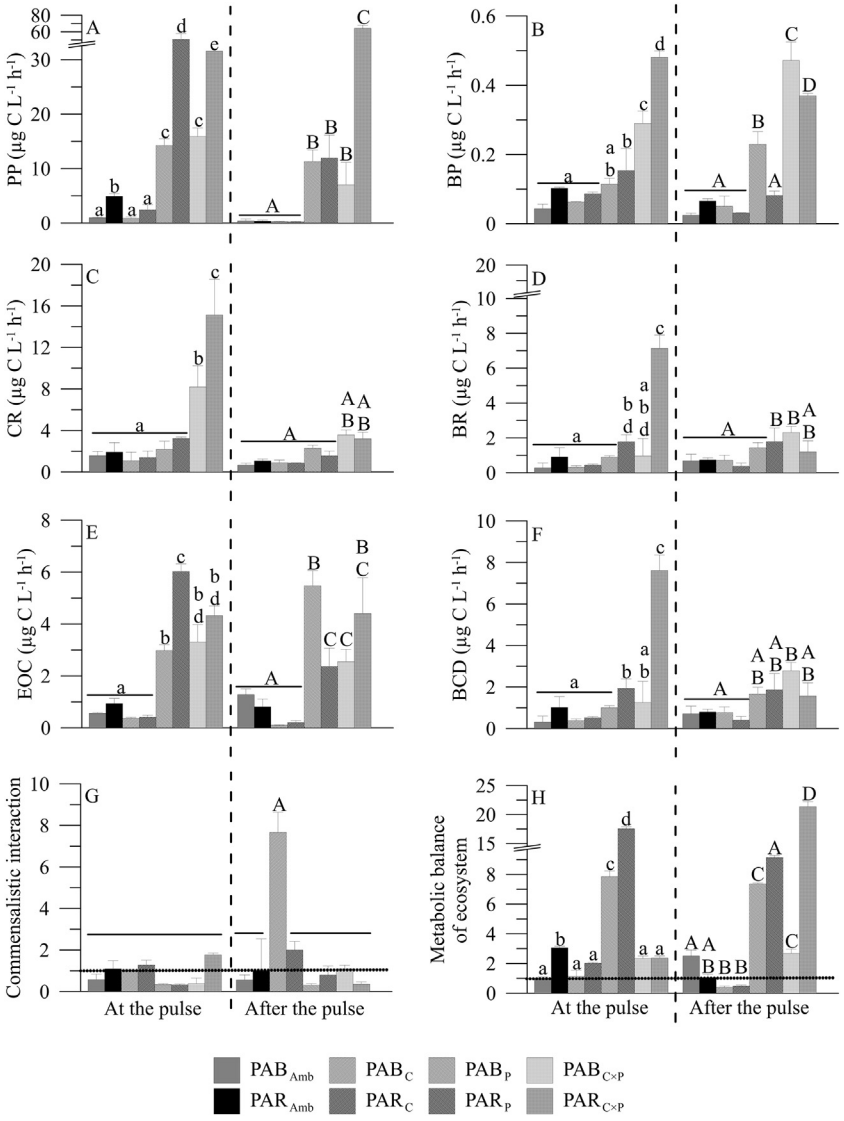

Fig. 3. (A) Primary production (PP, in µg C L^{-1} h^{-1}), (B) bacterial production (BP, in µg C L^{-1} h^{-1}), (C) community (CR) and (D) and bacterial respiration (BR) (in µg C L^{-1} h^{-1}), (E) excretion of organic carbon (EOC, in µg C L^{-1} h^{-1}), (F) bacterial carbon demand (BCD, in µg C L^{-1} h^{-1}), (G) commensalistic interaction (BCD:EOC ratio), and (H) metabolic balance of ecosystem (primary production:respiration ratio) at the pulse, and after the pulse period in each radiation (PAB [>280 nm] and PAR [>400 nm]) and nutrients (ambient, carbon [C], phosphorus [P] and C × P) treatment. The bars represent mean values of three replicates and lines in top of the bars are the standard deviation. Letters indicate differences among treatments by Tukey HSD post hoc test.

mechanisms underlying this cascading response across different organizational levels (Fig. 7).

First, the question arises concerning which compartment of the microbial food web would be most resistant to interacting stressors. Mixotrophs constituted the functional group most resistant to the simultaneous action of UVR × C × P. This resistance could result from the ability of mixotrophs to combine phototrophy and phagotrophy within a single cell (Mitra et al., 2016; Wilken et al., 2014), supporting the notion of a greater individual flexibility to cope with the environmental disturbance (Shade et al., 2012). In contrast to mixotrophs, phototrophs increased their resilience under the UVR × C × P scenario (Fig. 7). The resilience of phototrophs was tightly connected with a reduced metabolic resistance, reflected in greater PP, an improved sestonic P content, and a balanced C:P ratio under this scenario. Thus, in contrast to findings reported by Hillebrand et al. (2018), we found a significant negative correlation between compositional (i.e. diversity) and metabolic (i.e. PP) resilience—that is, an increase in the compositional resilience was coupled with reductions in the metabolic resilience. This inverse relationship could have resulted from functional instability (i.e. less resistance or resilience of PP) associated to higher PP rates with greater numbers of interacting stressors (i.e. UVR, UVR × C, UVR × P, and UVR × C × P).

Heterotrophic bacteria, however, was the community with the least stability under UVR × C × P, since their resistance weakened and did not improve their resilience. These results support previous findings by Shade et al. (2012) in which bacteria seems to be highly sensitive to pulse disturbances (i.e. low resistance), and have a weak recovery ability to such events (i.e. low resilience). The key mechanism for this reduced stability could be the high BR rates, as metabolic costs, to face with damaging stressors (e.g. UVR). Thus, high cellular stress could undermine their ability for nutrient uptake (Seymour et al., 2017), making them worse competitors than phytoplankton in such highly UVR-stressed ecosystems (Carrillo et al., 2008b; Sereda et al., 2011; Yuan et al., 2011). The tradeoff between cell self-preservation from environmental stress and nutritional competence is likely the major selective influence behind such responses and the main cause of meager bacterial development and of the paucity of ciliates and HNFs in Lake La Caldera (Medina-Sánchez et al., 2004; Medina-Sánchez et al., 2013). This proposal is also in line with previous experimental and observational studies in oligotrophic ecosystems showing no clear effect of nutrients or

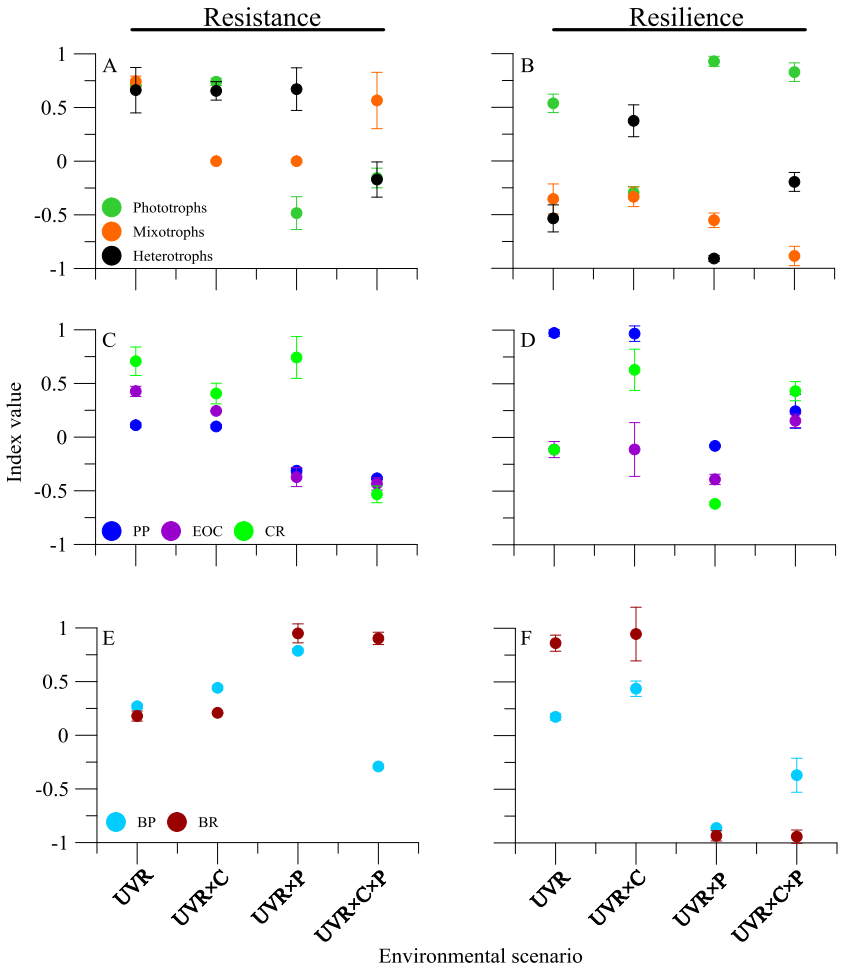

Fig. 4. Index values of resistance and resilience of photo-, mixo- and heterotrophs (A, B), primary production (PP), excreted organic carbon (EOC), community respiration (CR) (C, D), and bacterial production (BP) and respiration (BR) (E, F) under the four environmental scenarios: ultraviolet radiation (UVR), UVR and carbon (C) (UVR × C), UVR and phosphorus (UVR × P) and UVR × C × P environmental scenarios. Symbols represent mean values of three replicates and lines the standard deviation calculated by error propagation. Letters indicate differences among treatments by Tukey HSD post hoc test.

UVR on bacteria biomass (Cabrerizo et al., 2017; Carrillo et al., 2008a; Rojo et al., 2017).

Second, it might be asked how the stability of the commensalistic phytoplankton-bacteria interaction could be altered under interacting stressors. The joint pulses of C and P under UVR maintained the commensalism, and therefore the BCD:EOC ratio was <1 at the pulse to ~1 after that period (Fig. 3G). This finding indicates that despite the increased BP and BR rates under the UVR × C × P scenario, the C supply by phytoplankton (EOC) supported the bacterial C demands. The phytoplankton-bacteria coupling has been consistently reported in oligotrophic freshwater (Durán et al., 2016; González-Olalla et al., 2018) and marine (Fouilland et al., 2014) ecosystems. This response made

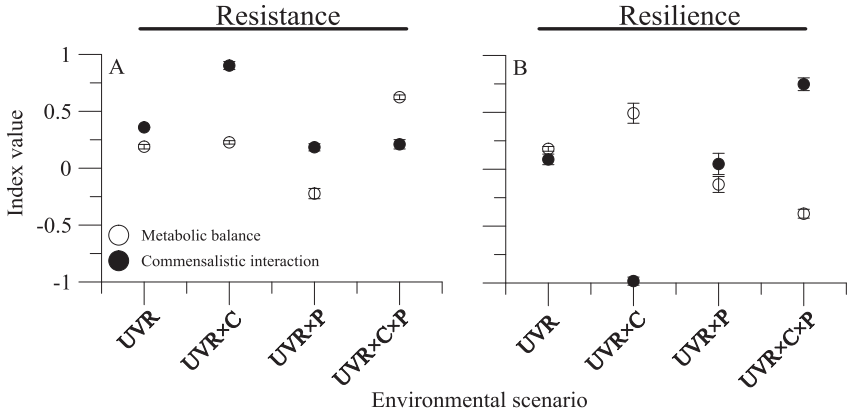

Fig. 5. Index values of resistance (A) and resilience (B) of the commensalistic interaction (bacterial carbon demand:excreted organic carbon ratio) and metabolic balance of ecosystem (primary production:respiration ratio) under the four environmental scenarios: ultraviolet radiation (UVR), UVR and carbon (C) (UVR × C), UVR and phosphorus (UVR × P) and UVR × C × P environmental scenarios. Symbols represent mean values of three replicates and lines the standard deviation calculated by error propagation. Letters indicate differences among treatments by Tukey HSD post hoc test.

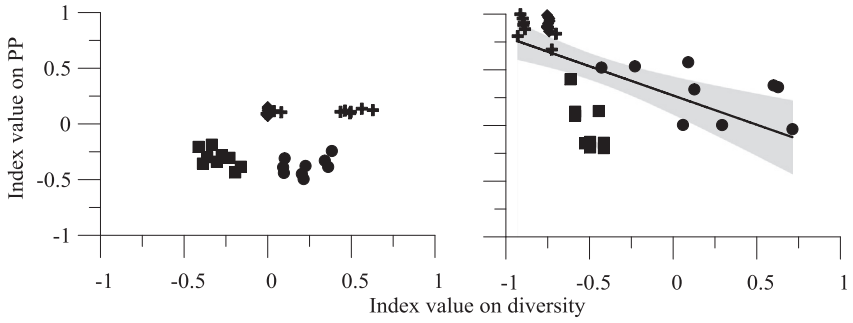

Fig. 6. Relationship between resistance (A) and resilience (B) of diversity versus primary production (PP) under the four environmental scenarios; ultraviolet radiation (UVR), UVR and carbon (C) (UVR × C), UVR and phosphorus (UVR × P) and UVR × C × P. Symbols represent the combination of all experimental replicates, solid line the linear regression fit model, and dashed lines the 95% interval confidence.

the commensalistic interaction highly stable due primarily to high resilience (ca. 0.75; Fig. 7). Moreover, phytoplankton can exert a resource-based control on bacteria through the regulation of extracellular C release. This strategy, and the well-known bacterial dependence of this labile C, may enable phytoplankton to outcompete bacteria for nutrients in high-mountain lakes (Medina-Sánchez et al., 2002; Villar-Argaiz et al., 2002) and boreal peatlands (Wyatt and Turetsky, 2015). This phytoplanktonic strategy is consistent with the steadiness of the bacterial community, a characteristic of this ecosystem (Cabrerizo et al., 2017; Carrillo et al., 2006; Medina-Sánchez et al., 2004). This underlines the increasingly recognized role of cross-kingdom interaction in shaping plankton communities and their dynamics, as well as the C fluxes in ecosystems (Cirri and Pohnert, 2019).

A final question might be raised concerning how these changes in the microbial food-web stability might propagate to the metabolic balance of the ecosystem under future environmental scenarios. The interaction between C, P, and UVR strengthened the resistance but weakened the resilience of the ecosystem's metabolic balance (Fig. 7). Thus, partially in agreement with our hypothesis, stronger resistance suggests robustness of the ecosystem to withstand the impacts of global-change, and could promote the sustained net autotrophy recently reported in this model oligotrophic ecosystem (Cabrerizo et al., 2017; Dorado-García et al., 2014). The high C-sink capacity of the ecosystem coupled with a high resistance of PP:R under future complex environmental scenarios is supported by three strong pieces of evidence outlined above: 1) greater PP and development (and the dominance) of phototrophs, which fueled the entire microbial food web (i.e. bacteria and mixotrophs); 2) low resilience of bacterial metabolism (BP and BR); and 3) the maintenance of stability of the commensalistic phytoplankton-bacteria interaction.

Notably, only the UVR × C scenario, which triggered a disconnection between resistance (moderate) and resilience (the highest) for PP:R, promoted shifts in the metabolic balance in Lake La Caldera towards the heterotrophy. More R together with less PP (i.e. decreasing C incorporation) was also reflected in diminished extracellular C release by phytoplankton after the pulse period, leading to a phytoplankton-bacteria uncoupling (BCD:EOC > 1). These results are consistent with previous evidence reported by Hanson et al. (2003) in temperate lakes indicating that allochthonous inputs alone (e.g. C) may influence lake metabolism, as this is strongly correlated with high R and low PP.

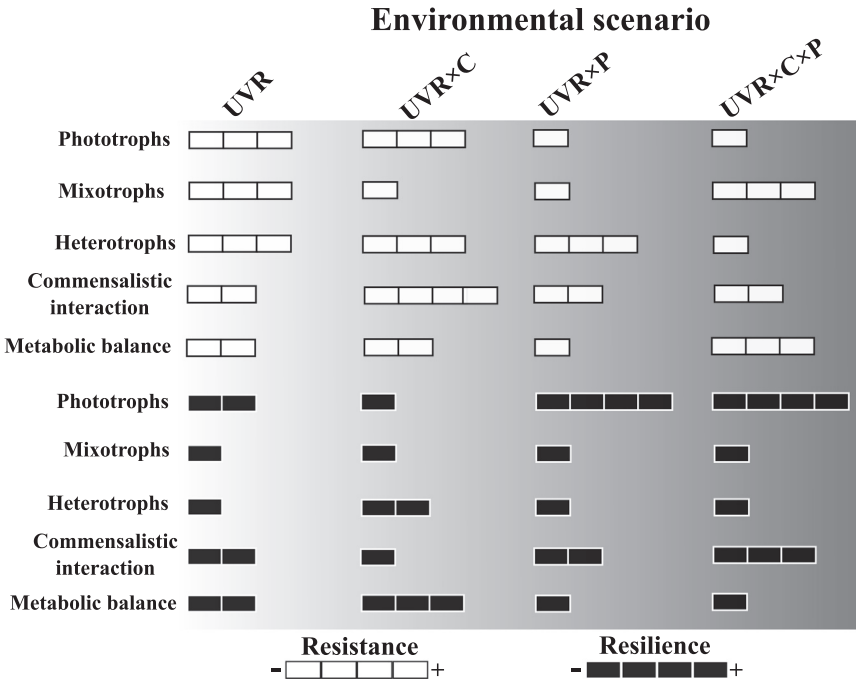

Fig. 7. Graphical scheme of the relative magnitude of the resistance and resilience indexes for functional groups (photo-, mixo- and heterotrophs), commensalistic interaction (bacterial carbon demand:excreted organic carbon ration [BCD:EOC ratio]) and metabolic balance of ecosystem (primary production:respiration [PP:R] ratio) under the four environmental scenarios: ultraviolet radiation (UVR) and their interaction with carbon (C), phosphorus (P) and C × P. Note that white and black bars denote a gradient between minima (−) and maxima (+) values, with – being resistance or resilience values between −1 and 0, and + values >0.66 to 1. Intermediate rectangles represent limits between 0–0.33 and 0.33–0.66.

Therefore, a disconnection between resistance and resilience at a metabolic level may lead the ecosystem to act as a C source to the atmosphere.

In conclusion, our research adds to recent studies emphasizing the need to evaluate multiple dimensions of stability for separating the responses of the community composition (compositional stability) of ecosystem processes (metabolic stability) (Hillebrand et al., 2018; Hoover et al., 2014; Gulzow et al., 2017). In addition, for first time, we quantify the interactive effect of multiple stressors on the multifaceted aspects of the stability of ecosystems in a global-change context. Our results show that, under the most complex environmental scenario, the high resilience of phototrophs (favoring their predominance over mixo- and heterotrophs) as well as the high resilience of the commensalistic interaction may reinforce the stability of the microbial food web. Finally, the high resistance of the PP:R ratio, which was related mainly to the greater resistance of BR, appears to help maintain the ecosystem C-sink capacity. Therefore, studies with complex designs such as the present one open the way to more realistic knowledge about how instability of underlying biological processes may generate shifts that are currently occurring in worldwide ecosystems.

Acknowledgements

We thank S. Rosillo, E. Jiménez-Coll, G. Herrera, I. Dorado-García, S. Velasco-Ayuso and J. Rodríguez Huertas for their help in different stages of the experimental setup, sampling and sample analyses. C. Durán is acknowledged by perform the flow cytometry analyses, and D. Nesbitt by English-writing assistance. We are also indebted to the staff of Sierra Nevada National Park for permission to work in Lake La Caldera. Comments and suggestions by the Editor Dr. Daniel Wunderlin and two anonymous reviewers on previous versions of the manuscript are deeply acknowledged. This study was supported by the Ministerio de Economía y Competitividad (MINECO) and Fondo Europeo de Desarrollo Regional (FEDER) (MICROSENS - CGL2011-23681 to PC and METAS - CGL2015-67682-R to JMMS and PC), Junta de Andalucía (P12-RNM-327 to MVA and P09-RNM-5376 to JMMS). M.J.C. was supported by a “Contrato Puente” contract funded by METAS project and the 7th Plan propio from University of Granada (FP7/2017), and by a Juan de la Cierva postdoctoral fellowship (FJCI-2017-32318) from the Ministry of Science, Innovation and Universities. Authors declare no conflict of interest.

Author contributions

JMMS, MVA and PC conceived the study. MJC, JMMS, MVA and PC designed and performed the study. MJC analyzed the samples and data, made tables and figures, and wrote the manuscript. PC, JMMS and MVA provided the funding and tools. All authors contributed substantially to the manuscript drafts and gave final approval for publication.

Appendix A. Supplementary data

Supplementary data to this article can be found online at https://doi.org/10.1016/j.scitotenv.2019.07.173.

References

Allison, S.D., Martiny, J.B.H., 2008. Resistance, resilience, and redundancy in microbial communities. Proc. Natl. Acad. Sci. 105, 11512–11519.
APHA, 2017. Standard Methods for the Examination of Water and Wastewater. American Public Health Association, Washington.
Ask, J., Karlsson, J., Jansson, M., 2012. Net ecosystem production in clear-water and brown-water lakes. Glob. Biogeochem. Cycles 26, GB1017.
Baert, J.M., De Laender, F., Sabbe, K., Janssen, C.R., 2016. Biodiversity increases functional and compositional resistance, but decreases resilience in phytoplankton communities. Ecology 97, 3433–3440.
Benner, R., Strom, M., 1993. A critical evaluation of the analytical blank asociated with DOC measurements by high-temperature catalytic oxidation. Mar. Chem. 41, 153–160.
Bergström, A.-K., Karlsson, J., Karlsson, D., Vrede, T., 2018. Contrasting plankton stoichiometry and nutrient regeneration in northern arctic and boreal lakes. Aquat. Sci. 80, 24.
Bogard, M.J., Finlay, K., Waiser, M.J., Tumber, V.P., Donald, D.B., Wiik, E., Simpson, G.L., Del Giorgio, P.A., Leavitt, P.R., 2017. Effects of experimental nitrogen fertilization on planktonic metabolism and CO_2 flux in a hypereutrophic hardwater lake. PLoS One 12, e0188652.
Cabrerizo, M.J., Medina-Sánchez, J.M., Dorado-García, I., Villar-Argaiz, M., Carrillo, P., 2017. Rising nutrient-pulse frequency and high UVR strengthen microbial interactions. Sci. Rep. 7, 43615.
Carrillo, P., Medina-Sánchez, J.M., Villar-Argaiz, M., 2002. The interaction of phytoplankton and bacteria in a high mountain lake: importance of the spectral composition of solar radiation. Limnol. Oceanogr. 47, 1294–1306.
Carrillo, P., Medina-Sánchez, J.M., Villar-Argaiz, M., Delgado-Molina, J.A., Bullejos, F.J., 2006. Complex interactions in microbial food webs: stoichiometric and functional approaches. Limnetica 25, 189–204.
Carrillo, P., Delgado-Molina, J.A., Medina-Sánchez, J.M., Bullejos, F.J., Villar-Argaiz, M., 2008a. Phosphorus inputs unmask negative effects of ultraviolet radiation on algae in a high mountain lake. Glob. Chang. Biol. 14, 423–439.
Carrillo, P., Villar-Argaiz, M., Medina-Sánchez, J.M., 2008b. Does microorganism stoichiometry predict microbial food web interactions after a phosphorus pulse. Microb. Ecol. 56, 350–363.
Carrillo, P., Medina-Sánchez, J.M., Durán, C., Herrera, G., Villafañe, V.E., Helbling, E.W., 2015. Synergistic effects of UVR and simulated stratification on commensalistic algal-bacterial relationship in two optically contrasting oligotrophic Mediterranean lakes. Biogeosciences 12, 697–712.
Cirri, E., Pohnert, G., 2019. Algae-bacteria interactions that balance the planktonic microbiome. New Phytol. 223, 100–106.
Danger, M., Daufresne, T., Lucas, F., Pissard, S., Lacroix, G., 2008. Does Liebig's law of the minimum scale up from species to communities? Oikos 117, 1741–1751.
de Vries, F.T., Liiri, M.E., Bjørnlund, L., Bowker, M.A., Christensen, S., Setälä, H.M., Bardgett, R.D., 2012. Land use alters the resistance and resilience of soil food webs to drought. Nat. Clim. Chang. 2, 276–280.
Degerman, R., Lefébure, R., Byström, P., Bamstedt, U., Larsson, U., Andersson, A., 2018. Food web interactions determine energy transfer efficiency and top consumer responses to inputs of dissolved organic carbon. Hydrobiologia 805, 131–146.
del Giorgio, P.A., Cole, J.J., 1998. Bacterial growth efficiency in natural aquatic systems. Annu. Rev. Ecol. Syst. 29, 503–541.
Donohue, I., Hillebrand, H., Montoya, J.M., Petchey, O.L., Pimm, S.L., Fowler, M.S., Healy, K., Jackson, A.L., Lurgi, M., McClean, D., O'Connor, N.E., O'Gorman, E.J., Yang, Q., 2016. Navigating the complexity of ecological stability. Ecol. Lett. 19, 1172–1185.
Dorado-García, I., Medina-Sánchez, J.M., Herrera, G., Cabrerizo, M.J., Carrillo, P., 2014. Quantification of carbon and phosphorus co-limitation in bacterioplankton: new insights on an old topic. PLoS One 9, e99288.
Dudgeon, D., Arthington, A.H., Gessner, M.O., Kawabata, Z.-I., Knowler, D.J., Lévêque, C., Naiman, R.J., Prieur-Richard, A.-H., Soto, D., Stiassny, M.L.J., Sullivan, C.A., 2006. Freshwater biodiversity: importance, threats, status and conservation challenges. Biol. Rev. 81, 163–182.
Durán, C., Medina-Sánchez, J.M., Herrera, G., Carrillo, P., 2016. Changes in the phytoplankton-bacteria coupling triggered by joint action of UVR, nutrients, and warming in Mediterranean high-mountain lakes. Limnol. Oceanogr. 61, 413–429.
Flöder, S., Hillebrand, H., 2012. Species traits and species diversity affect community stability in a multiple stressor framework. Aquat. Biol. 17, 197–209.
Fouilland, E., Tolosa, I., Bonnet, D., Bouvier, C., Bouvy, M., Got, P., Le Floc'h, E., Mostajir, B., Roques, C., Sempéré, R., Sime-Ngando, T., Vidussi, F., 2014. Bacterial carbon dependence on freshly produced phytoplankton exudates under different nutrient availability and grazing pressure conditions in coastal marine waters. FEMS Microbiol. Ecol. 87, 757–769.
Fuhrman, J.A., Azam, F., 1982. Thymidine incorporation as a measure of heterotrophic bacterioplankton production in marine surface waters: evaluation and field results. Mar. Biol. 66, 109–120.
Garnier, A., Pennekamp, F., Lemoine, M., Petchey, O.L., 2017. Temporal scale dependent interactions between multiple environmental disturbances in microcosm ecosystems. Glob. Chang. Biol. 23, 5237–5248.
González-Olalla, J.M., Medina-Sánchez, J.M., Lozano, I.L., Villar-Argaiz, M., Carrillo, P., 2018. Climate-driven shifts in algal-bacterial interaction of highmountain lakes in two years spanning a decade. Sci. Rep. 8, 10278.
Gulzow, N., Muijsers, F., Ptacnik, R., Hillebrand, H., 2017. Functional and structural stability are linked in phytoplankton metacommunities of different connectivity. Ecography 40, 719–732.
Hanson, P.C., Bade, D.L., Carpenter, S.R., Kratz, T.K., 2003. Lake metabolism: relationships with dissolved organic carbon and phosphorus. Limnol. Oceanogr. 48, 1112–1119.
Hillebrand, H., Dürselen, C.D., Kirschtel, D., Pollingher, U., Zohary, T., 1999. Biovolume calculation for pelagic and benthic microalgae. J. Phycol. 35, 403–424.
Hillebrand, H., Langenheder, S., Lebret, K., Lindström, E., Östman, Ö., Striebel, M., 2018. Decomposing multiple dimensions of stability in global change experiments. Ecol. Lett. 21, 21–30.
Hoover, D.L., Knapp, A.K., Smith, M.D., 2014. Resistance and resilience of a grassland ecosystem to climate extremes. Ecology 95, 2646–2656.
IPCC, 2013. Climate Change. The Physical Science Basis. Cambridge University Press, New York, USA.
Jeffrey, S.W., Humphrey, G.F., 1975. New spectrophotometric equations for determining chlorophylls a, b, c 1 and c 2 in higher plants, algae and natural phytoplankton. Biochem. Physiol. Pflanz. 167, 191–194.
Kamiya, E., Izumiyama, S., Nishimura, M., Mitchell, J.G., Kogure, K., 2007. Effects of fixation and storage on flow cytometric analysis of marine bacteria. J. Oceanogr. 63, 101–112.

Mayali, X., 2018. Metabolic interactions between bacteria and phytoplankton. Front. Microbiol. 9, 727.
Medina-Sánchez, J.M., Villar-Argaiz, M., Carrillo, P., 2002. Modulation of the bacterial response to spectral solar radiation by algae and limiting nutrients. Freshw. Biol. 47, 2191–2204.
Medina-Sánchez, J.M., Villar-Argaiz, M., Carrillo, P., 2004. Neither with nor without you: a complex algal control on bacterioplankton in a high mountain lake. Limnol. Oceanogr. 49, 1722–1733.
Medina-Sánchez, J.M., Delgado-Molina, J.A., Bratbak, G., Bullejos, F.J., Carrillo, P., 2013. Maximum in the middle: nonlinear response of microbial plankton to ultraviolet radiation and phosphorus. PLoS One 8, e60223.
Mendonça, R., Müller, R.A., Clow, D., Verpoorter, C., Raymond, P., Tranvik, L.J., Sobek, S., 2018. Organic carbon burial in global lakes and reservoirs. Nat. Commun. 8, 1694.
Mitra, A., Flynn, K.J., Tillmann, U., Raven, J.A., Caron, D., Stoecker, D.K., Not, F., Hansen, P.J., Hallegraeff, G., Sanders, R., Wilken, S., McManus, G., Johnson, M., Pitta, P., Vage, S., Berge, T., Calbet, A., Thingstad, F., Jin Jeong, H., Burkholder, J., Glibert, P.M., Granéli, E., Lundgren, V., 2016. Defining planktonic protist functional groups on mechanisms for energy and nutrient acquisition: incorporation of diverse mixotrophic strategies. Protist 167, 106–120.
Morales-Baquero, R., Pulido-Villena, E., Reche, I., 2006. Atmospheric inputs of phosphorus and nitrogen to the southwest Mediterranean region: biogeochemical responses of high mountain lakes. Limnol. Oceanogr. 57, 830–837.
Morán, X.A.G., Estrada, M., Gasol, J.M., Pedrós-Alió, C., 2002. Dissolved primary production and the strength of phytoplankton-bacterioplankton coupling in contrasting marine regions. Microb. Ecol. 44, 217–223.
Mostajir, B., Amblard, C., Buffan-Dubau, E., De Wit, R., Lensi, R. & Sime-Ngando, T. (2015) Microbial food webs in aquatic and terrestrial ecosystems. Environmental Microbiology: Fundamentals and Applications (eds J. C. Bertrand, P. Caumette, P. Lebaron, R. Matheron, P. Normand & T. Sime-Ngando), pp. 993. Springer, Dordrecht.
Orwin, K.H., Wardle, D.A., 2004. New indices for quantifying the resistance and resilience of soil biota to exogenous disturbances. Soil Biol. Biochem. 36, 1907–1912.
Posch, T., Loferer-Krößbacher, M., Gao, G., Alfreider, A., Pernthaler, J., Psenner, R., 2001. Precision of bacterioplankton biomass determination: a comparison of two fluorescent dyes, and of allometric and linear volume-to-carbon conversion factors. Aquat. Microb. Ecol. 25, 55–63.
Ramanan, R., Kim, B.-H., Cho, D.-H., Oh, H.-M., Kim, H.-S., 2016. Algae–bacteria interactions: evolution, ecology and emerging applications. Biotechnol. Adv. 34, 14–29.
Reche, I., Pulido-Villena, E., Conde-Porcuna, J.M., Carrillo, P., 2001. Photoreactivity of dissolved organic matter from high-mountain lakes of Sierra Nevada, Spain. Arct. Antarct. Alp. Res. 33, 426–434.
Rocha, O., Duncan, A., 1985. The relationship between cell carbon and cell volume in freshwater algal species used in zooplankton studies. J. Plankton Res. 7, 279–294.
Rojo, C., Herrera, G., Medina-Sánchez, J.M., Villar-Argaiz, M., Durán, C., Carrillo, P., 2017. Are the small-sized plankton communities of oligotrophic ecosystems resilient to UVR and P pulses? Freshw. Sci. 36, 760–773.
Russell, B.D., Connell, S.D., 2014. Ecosystem resilience and resistance to climate change. In: Freedman, B. (Ed.), Global Environmental Change. Handbook of Global Environmental Pollution. Springer, Dordrecht, pp. 133–139.
Sereda, J.M., Vandergucht, D.M., Hudson, J.J., 2011. Disruption of planktonic phosphorus cycling by ultraviolet radiation. Hydrobiologia 665, 205–217.
Seymour, J.R., Amin, S.A., Raina, J.-B., Stocker, R., 2017. Zooming in on the phycosphere: the ecological interface for phytoplankton–bacteria relationships. Nat. Microbiol. 2, 17065.
Shade, A., Read, J.S., Welkie, D.G., Kratz, T.K., Wu, C.H., McMahon, K.D., 2011. Resistance, resilience and recovery: aquatic bacterial dynamics after water column disturbance. Environ. Microbiol. 13, 2752–2767.
Shade, A., Peters, H., Allison, S.D., Baho, D.L., Berga, M., Bürgmann, H., Huber, D.H., Langenheder, S., Lennon, J.T., Martiny, J.B.H., Matulich, K.L., Schmidt, T.M., Halndelsman, J., 2012. Fundamentals of microbial community resistance and resilience. Front. Microbiol. 3, 417.
Shannon, C.E., Weaver, W., 1949. The Mathematical Theory of Communication. University of Illinois Press, Urbana, USA.
Steemann Nielsen, E., 1952. The use of radio-active carbon (C^{14}) for measuring organic production in the sea. J. Cons. Int. Explor. Mer 18, 117–140.
Straškrabová, V., Callieri, C., Carrillo, P., Cruz-Pizarro, L., Fott, J., Hartman, P., Macek, M., Medina-Sánchez, J.M., Nedoma, J., Šimek, K., 1999. Investigations on pelagic food webs in mountain lakes - aims and methods. J. Limnol. 58, 77–87.
Vidal, L.O., Granéli, W., Daniel, C.B., Heiberg, L., Roland, F., 2011. Carbon and phosphorus regulating bacterial metabolism in oligotrophic boreal lakes. J. Plankton Res. 33, 1747–1756.
Villar-Argaiz, M., Medina-Sánchez, J.M., Cruz-Pizarro, L., Carrillo, P., 2001. Inter- and intra-annual variability in the phytoplankton community of a high mountain lake: the influence of external (atmospheric) and internal (recycled) sources of phosphorus. Freshw. Biol. 46, 1017–1034.
Villar-Argaiz, M., Medina-Sánchez, J.M., Carrillo, P., 2002. Microbial plankton response to contrasting climatic conditions: insights from community structure, productivity and fraction stoichiometry. Aquat. Microb. Ecol. 29, 253–266.
Villar-Argaiz, M., Balseiro, E.G., Modenutti, B.E., Souza, M.S., Bullejos, F.J., Medina-Sánchez, J.M., Carrillo, P., 2018. Resource versus consumer regulation of phytoplankton: testing the role of UVR in a Southern and Northern hemisphere lake. Hydrobiologia 816, 107–120.
Wilken, S., Schuurmans, J.M., Matthijs, H.C.P., 2014. Do mixotrophs grow as photoheterotrophs? Photophysiological acclimation of the chrysophyte *Ochromonas danica* after feeding. New Phytol. 204, 882–889.
Wyatt, T., Turetsky, M.R., 2015. Algae alleviate carbon limitation of heterotrophic bacteria in a boreal peatland. J. Ecol. 103, 1165–1171.
Yuan, X., Yin, K., Harrison, P.J., Zhang, J., 2011. Phytoplankton are more tolerant to UV than bacteria and viruses in the northern South China Sea. Aquat. Microb. Ecol. 65, 117–128.
Zubkov, M.V., Burkill, P.H., 2006. Syringe pumped high speed flow cytometry of oceanic phytoplankton. Cytometry A 69, 1010–1019.
Zubkov, M.V., Burkill, P.H., Topping, J.N., 2007. Flow cytometric enumeration of DNA-stained oceanic planktonic protists. J. Plankton Res. 29, 79–86.